



*Transactions, SMiRT-26*  
Berlin/Potsdam, Germany, July 10-15, 2022  
Division IX

## **INVESTIGATION OF THE RADIOLOGICAL IMPACT OF A FORKLIFT TRUCK FIRE ON RADIOACTIVE WASTE STORED IN 20' CONTAINERS**

**J. Struve<sup>1</sup>, M. Brüger<sup>2</sup>, L. Landwehr<sup>3</sup>**

<sup>1</sup> Head of Fire Safety, TUEV NORD EnSys, Hamburg, Germany (jstruve@tuev-nord.de)

<sup>2</sup> Technical Expert Hydraulic Analyses and Fluid Dynamics, TUEV NORD EnSys, Hamburg, Germany

<sup>3</sup> Head of Radioecology and Water Law, TUEV NORD EnSys, Hamburg, Germany

### **ABSTRACT**

As part of the decommissioning and dismantling process of nuclear facilities, waste is stored in various storage containers. During the handling of these storage containers, a fire may occur and radionuclides may be released from the containers because of fire. In this paper, we show how to perform an impact assessment for this scenario. For this purpose, we first assume three possible fire events, which differ in terms of the timing of extinguishing measures. Based on the corresponding fire temperature curves, we derive the boundary conditions for a heat penetration calculation. Based on the results of heat penetration calculations using the finite element method, we can use correlation functions to determine the release fractions of selected radionuclides. To estimate the dose exposure, we perform a dispersion calculation using a Lagrangian particle trajectory model. It turns out that a significant proportion of the release occurs after the end of the fire and that early firefighting can contribute to reduce the release significantly.

### **INTRODUCTION**

During the decommissioning of nuclear facilities, radioactive waste is produced by dismantling processes and stored in different storage containers depending on the type of radioactive waste. In the context of the German waste management strategy, a distinction must be made between waste containers that meet the requirements of the Federal Office for Radiation Protection (BFS) (2010, 2010a, 2010b) and waste containers that do not meet these requirements. The latter are, for example, 20' containers used in the context of interim storage for short term temporary storage before the final conditioning steps. According to ESK (2021), all permanent and temporary fire loads (e.g. forklifts in the course of transport operations) must be taken into account in the investigation of potential thermal effects on stored containers as part of the safety analysis. While permanent fire loads are largely avoided in order to reduce the fire hazard, temporary fire loads can occur in particular during transport operations and can have a thermal effect on the stored containers in the immediate vicinity in the event of a fire. The fire of a transport vehicle (e.g. forklift truck) represents a corresponding scenario.

The release of radioactive substances from storage containers due to thermal effects depends on the heat flow that heats up the container and on the duration of the fire. The heat conduction within the container is influenced by the design of the container and the thermal properties of its internals, and finally quite importantly by the properties of the radioactive waste itself. The heating of the radioactive waste can lead to the release of radioactivity, which can be attributed to several processes. For example, according to ESK (2021), the processes of evaporation, pyrolysis and sublimation must be considered. All these processes are highly dependent on the local temperature of the radioactive waste and other boundary conditions such as oxygen supply.

In addition, the temperature inside the radioactive waste and the release of radioactivity to the environment is influenced by the thermal insulation and the integrity of the storage container. Radioactive waste in a 20' container can heat up faster than radioactive waste stored in high-level storage containers (e.g. for fuel assemblies, etc.), which usually have better thermal insulation. For this reason, fire loads for 20' containers generally represent sensitive parameters. Therefore, the relevant boundary conditions must be determined for the respective scenario and possible fire progressions must be taken into account. In this context, the available fire protection infrastructure, e.g. the response times of the plant fire departments, can also play a relevant role.

In the present work, we will first determine a covering fire scenario and present a conservative fire curve for it. By means of thermal structural analyses with the finite element method, we perform the calculation of local temperature curves inside the radioactive waste with the required accuracy. Based on these curves, we use known correlations for release rates to integrate the radioactive release over time. Once the temperature distribution is known, the time-dependent release rate of radioactivity can be calculated and a potential total exposure for the population can be determined.

## SCENARIO MODELING

A general model that takes into account all affected sub-processes does not exist. In this respect, the calculation of the present scenario consists of different submodels, in which the result of submodel  $n$  is used as the source term in submodel  $n + 1$ . It is possible that the quality and complexity of the individual models deviate from each other. This must be taken into account when interpreting the results and, if necessary, when selecting model parameters. The individual partial steps (models) for the present case are shown in Fig. 1.

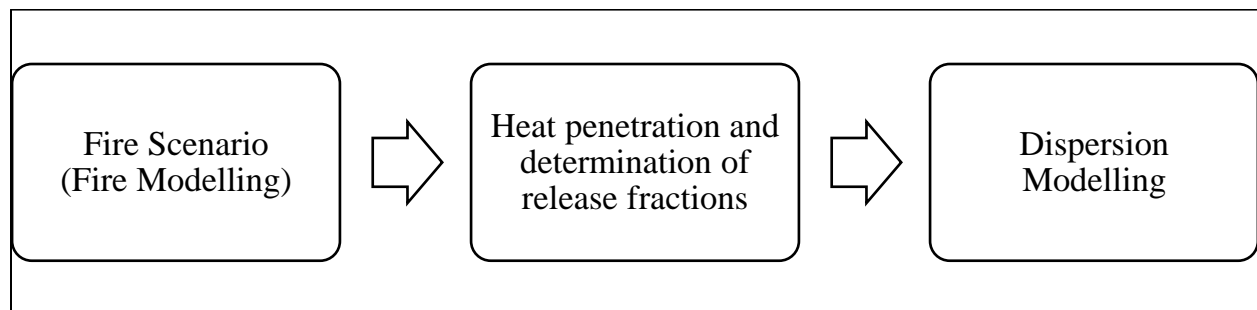


Figure 1. Sequence of the impact analysis based on three coupled models

### *Fire Scenario*

In the present case, we take the fire of a forklift truck as the dominating fire case. Such forklift trucks are often used in connection with transport and handling operations of 20' containers and usually represent the highest temporary fire load in storage areas. The type and size of these transport vehicles can vary greatly depending on the corresponding logistics concept. The main fire load of such a vehicle is represented by the operating fluids (e.g. diesel fuel, hydraulic oils) and the tires. For the purpose of this study, we assume that the fuel tank is damaged and that the corresponding pool is ignited. We also assume that this pool is located directly at the 20' container.

To measure the thermal impact of the pool fire, we use the hydrocarbon curve. This is a normalized temperature-time curve for fires of hydrocarbons, which was originally developed in the 1970s for industrial and off-shore plants. The course of the fire curve is calculated according to DIN EN 1991-1-2 (2010):

$$T_g = 1080 (1 - 0.325 e^{-1.67 t} - 0.675 e^{-2.5 t}) + 20, \quad (1)$$

where  $T_g$  describes the gas temperature in the fire room in °C and  $t$  the fire duration in minutes. For the present case, we consider three different scenarios. In the first two cases, existing fire protection boundary conditions (intervention of the plant fire department after 5 min or the public fire department after 10 min) are taken into account. In the third scenario, we assume a fire with a duration of 30 min. The different fire sequences are shown in Fig. 2. The extinguishing effect in scenarios 1 and 2 has been taken into account by an empirical factor from vfdb (2020). It should be noted that the application of the hydrocarbon curve in the present case is a very conservative assumption. In individual cases, specific investigations may lead to significantly lower temperatures.

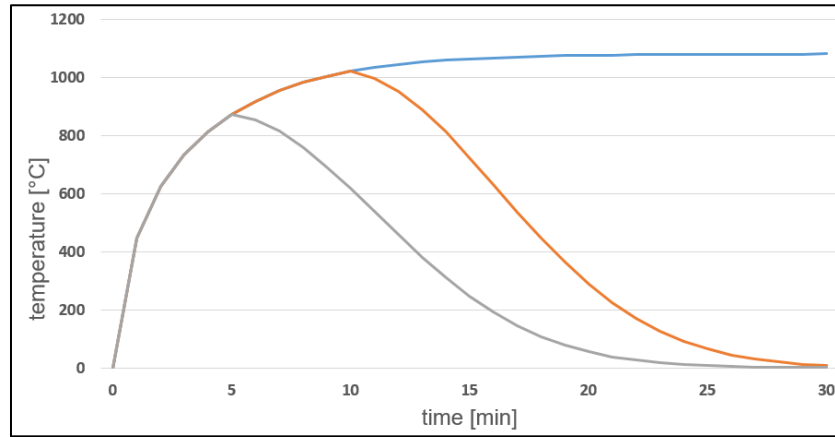


Figure 2. Considered fire progression curves: blue: without consideration of extinguishing measures; gray: consideration of a plant fire department (intervention time 5 min); orange: consideration of the public fire department (intervention time 10 min).

### ***Heat penetration and determination of release fractions***

The release of radioactive particles from waste packages under thermal load conditions is described by nuclide-specific, experimentally determined temperature-dependent release rates  $k(\theta)$ , depending on the mechanism for the release and therefore on the type of waste (metallic waste, mixed waste, concentrates). These release rates include both, the mass transfer into the gas phase and its transport process in the waste product. The release of the nuclides in the waste product can be described in a simplified way by the following differential equation for the nuclide concentration  $c(\vec{x}, t)$  in the waste product:

$$\frac{\partial c(\vec{x}, t)}{\partial t} = -k(\theta) \cdot c(\vec{x}, t) \quad (2)$$

To solve this equation, the time-dependent three-dimensional temperature distribution  $\theta(\vec{x}, t)$  in the waste product must be known. We calculate the temperature distribution using the finite element calculation program ANSYS 2021 R1. As a result of these calculations, in each finite element  $i$ ,  $i \in (1, \dots, NE)$  of the model describing the waste product the mean temperature  $\theta_{(i,j)}$  at time  $t_j \in (0, \dots, NT)$  is known. Accordingly, the above differential equation can be decomposed into a set of  $NE$  differential equations, where  $m_i = V_i \cdot c_i$  represents the mass of nuclides in the volume  $V_i$  of element  $i$ . Here, we assume that the nuclide under consideration is initially homogeneously distributed in the waste product, i.e., its concentration  $c$  is constant in the waste product before the thermal load.

$$\frac{dm_i}{dt} = -k(\theta_i(t)) \cdot m_i(t) \quad , \quad i = 1, \dots, NE \quad . \quad (3)$$

With the condition that the time difference between two calculation times is chosen so small that the change of the release rate  $k(\theta)$  can be neglected within a time step, we obtain as solutions for the differential equations the recursive calculation rule

$$m_{i,j} = m_{i,j-1} \cdot e^{-k(\theta_{i,j}) \cdot (t_j - t_{j-1})} \quad , \quad j = 1, \dots, NT \quad , \quad (4)$$

where  $m_{i,j}$  is the mass of the nuclide under consideration present in the volume  $V_i$  at time  $t_j$ . The total mass fraction  $f_{i,j}$  released in the volume  $V_i$  up to time  $t_j$  can then be calculated recursively with

$$f_{i,j} = \frac{m_{i,0} - m_{i,j}}{m_{i,0}} = 1 + (f_{i,j-1} - 1) \cdot e^{-k(\theta_{i,j}) \cdot (t_j - t_{j-1})} \quad . \quad (5)$$

This results in the total release fraction  $F_j$  or  $ARF$  at time  $t_j$ , respectively, with

$$F_j = \sum_i \frac{V_i}{V_{total}} \cdot f_{i,j} \quad . \quad (6)$$

Neglecting any retention capabilities of the package, in the following we consider the release fractions  $F_j$  as air release fractions  $ARF(t)$  to the environment. In practice, the release rate  $k(\theta)$  is usually determined only for a few so-called lead nuclides. The release fractions of the other nuclides, which are similar in their release behavior, are then determined via fixed numerical ratios from the results of the respective lead nuclides. In the following, we consider e.g. the release of radioactive nuclides from metals. We use for the lead nuclide Cs-137, analogous to Brüchner (2013), the correlation VEGA-1 derived from experimental data by Hidaka (2002)

$$k_{Cs}(\theta) = 1,44 \text{ min}^{-1} \cdot e^{-9280 K/\theta} \quad , \quad (7)$$

whose applicability was already demonstrated in Brüchner (2013) using the measured data from Boetsch (2005).

For our thermal analyses, we used a simplified 1/8 model of a 20' container, in which the waste is assumed to be homogeneous and to be surrounded only by a 3 mm thin layer of sheet metal. For our calculations, we chose scrap metal as the waste product, for which we assumed a homogenized density  $\rho = 3500 \text{ kg m}^{-3}$  and a thermal conductivity  $\lambda = 50 \text{ W m}^{-1} \text{ K}^{-1}$ . For our simulations, we divided the waste product uniformly into  $NE \approx 1.62 \cdot 10^5$  volume elements  $V_i$ . We chose a temperature  $\theta_{i,0} = 20 \text{ }^\circ\text{C}$ ,  $\forall i$  as the initial temperature of the waste package. For a calculation period of 30 min, we used the fire scenarios described above and simulated a heat exchange between environment and entire container surface by convection and radiation with the corresponding temperature-time histories of the fire. After 30 min, we assumed a linear decrease of the ambient temperature to  $20 \text{ }^\circ\text{C}$  within 5 min and considered a further cooling of the container surface at  $20 \text{ }^\circ\text{C}$  ambient temperature until a time of 24 h after the start of the fire. According to IAEA SSG (2012) the emissivity of the container surface was assumed as  $\epsilon_c = 0.8$  and that of the environment was assumed as  $\epsilon_a = 0.9$ . For the convective heat transfer at the container surface, according to IAEA SSG (2012) we assumed a coefficient  $\alpha = 10 \text{ W m}^{-2} \text{ K}^{-1}$  during the fire. For the cool-down period, we also applied  $\alpha = 10 \text{ W m}^{-2} \text{ K}^{-1}$  for reasons of simplification, which means that

the cooling processes in our simulations are generally overestimated. For the time step sizes  $t_j - t_{j-1}$  we used values between 30 s at the beginning of the simulation and 300 s at the end of the simulation.

### ***Dispersion Modelling***

With the determined release factors, we assess the potential dose for the population based on a model activity inventory and nuclide vector with a subsequent dispersion calculation. For this purpose, we adopted the activity inventory and nuclide vector from the ESK stress test (2013) for a high activity inventory of a 20' container with 4E11 Bq. For the nuclide distribution, we followed the vector of the ESK stress test (2013), but also took into account a 1% share of possibly occurring alphanuclides. This results in a vector of 69 % Co-60, 30 % Cs-137 and 1 % Am-241. Conservatively, we have assumed a release close to the ground and have not further considered a possible small thermal rise due to the short fire durations.

The subsequent dispersion calculation was performed with a Lagrangian particle trajectory model according to the VDI guideline 3945 part 3 (2020), which is implemented in the program code ARTM (2015). In this, individual trajectories are calculated for a large number of particles, in which a new position is calculated for each time step  $\tau$  according to Eq. 8.

$$\vec{x}_{new} = \vec{x}_{old} + \tau[\vec{V} + \vec{u} + \vec{U}] \quad (8)$$

Here  $\vec{V}$  is the mean wind velocity,  $\vec{u}$  the turbulence velocity varying with each time step and  $\vec{U}$  an additional or drift velocity to be considered if necessary, which describes e.g. the thermal superelevation.

We used the properties of a German nuclear power plant as model site and considered the resulting activity concentrations only from 100 m from the source point, because in reality the population is located outside a power plant site. The terrain and building influence was taken into account by the model. For the meteorological boundary conditions, in accordance with the guidelines for accident calculation BMI (1983) we considered

- the propagation direction of 12 sectors leading to the highest exposure,
- a wind speed of 1 m/s at a height of 10 m,
- the diffusion category leading to the highest total exposure, and
- 5 mm/h precipitation for diffusion categories C, D, and E and no precipitation for diffusion categories A, B, and F.

The subsequent dose calculation, which takes into account the calculated activity concentrations and depositions, was performed considering the exposure pathways and the formalism of the guidelines for accident calculation BMI (1983). For simplification, a respirable particle size of 10  $\mu\text{m}$  was assumed for the total released activity. The calculated dose is a follow-up dose until age of 70.

## **RESULTS**

From the individual temperature distributions at the respective time steps as shown in Figure 3, the integral release fractions are obtained according to the previously described approximation of the VEGA-1 correlation by temporal and spatial summation over all elements. Figures 4, 5 and 6 show the calculated time histories of the integral air release fractions ARF of scenarios 1, 2, and 3, respectively, together with the respective time histories of the flame temperature TF, a temperature at the surface of the waste TS (position marked in figure 3), and the temperature at the centre of the waste TI for the 4-h period.

The time histories show that for the fire durations considered here, a significant portion of the release occurs after the end of the pool fire, which is due to the delayed heat penetration into the interior of the waste. Thus, an early end of the fire can contribute significantly to the reduction of release not only by limiting the period of high temperatures, but also the maximum temperatures at the outer edge of the waste and the heat penetration into deeper layers. The relationships shown here as an example for one waste and one packaging type can in principle also be assumed for other waste packages. However, since the maximum release rate as well as the release duration strongly depend on the heat transport properties of the waste, the results presented here are not applicable to other types of waste and package. Instead, the calculations are to be made specifically for a waste type. Hereby, the element sizes as well as the time step widths may have to be adjusted. For example, for mixed wastes with significantly lower thermal conductivity, smaller elements should be used to compensate for the effect of the larger temperature gradient within each element volume. A corresponding independent convergence criterion for element size and time step size for the use of the approximation of the correlation VEGA-1 presented here still has to be worked out. Furthermore, the influence of different fire scenarios when using other correlations for the nuclide release, such as according to Gründler (1987), must be considered separately. Depending on the waste product, a distinction must be made between the release mechanisms of evaporation, pyrolysis and sublimation. From the above results, we derive three source terms for the fire, which we present in Table 1.

Table 1: Source terms for the dispersion modelling of the three scenarios

Nuclides	Entire Activity in Bq	Released Activity in Bq		
		Case 1 30-min-fire	Case 2 public fire department	Case 3 plant fire department
Co-60	2,76E+11	4,97E+07	3,04E+05	2,65E+03
Cs-137	1,20E+11	2,16E+07	1,32E+05	1,15E+03
Am-241	4,00E+09	7,20E+05	4,40E+03	3,84E+01

For our model site, diffusion category E leads to the highest exposure considering the northeastern wind direction. This results in a potential total exposure for the population of about 3E-1 mSv for Case 1. While we have the same nuclide vector, we only change the total released activity for Cases 2 and 3. Therefore, the exposure calculates from simple scaling. This results in a potential exposure of the population of about 2E-3 mSv for Case 2 and of about 2E-5 mSv for Case 3.

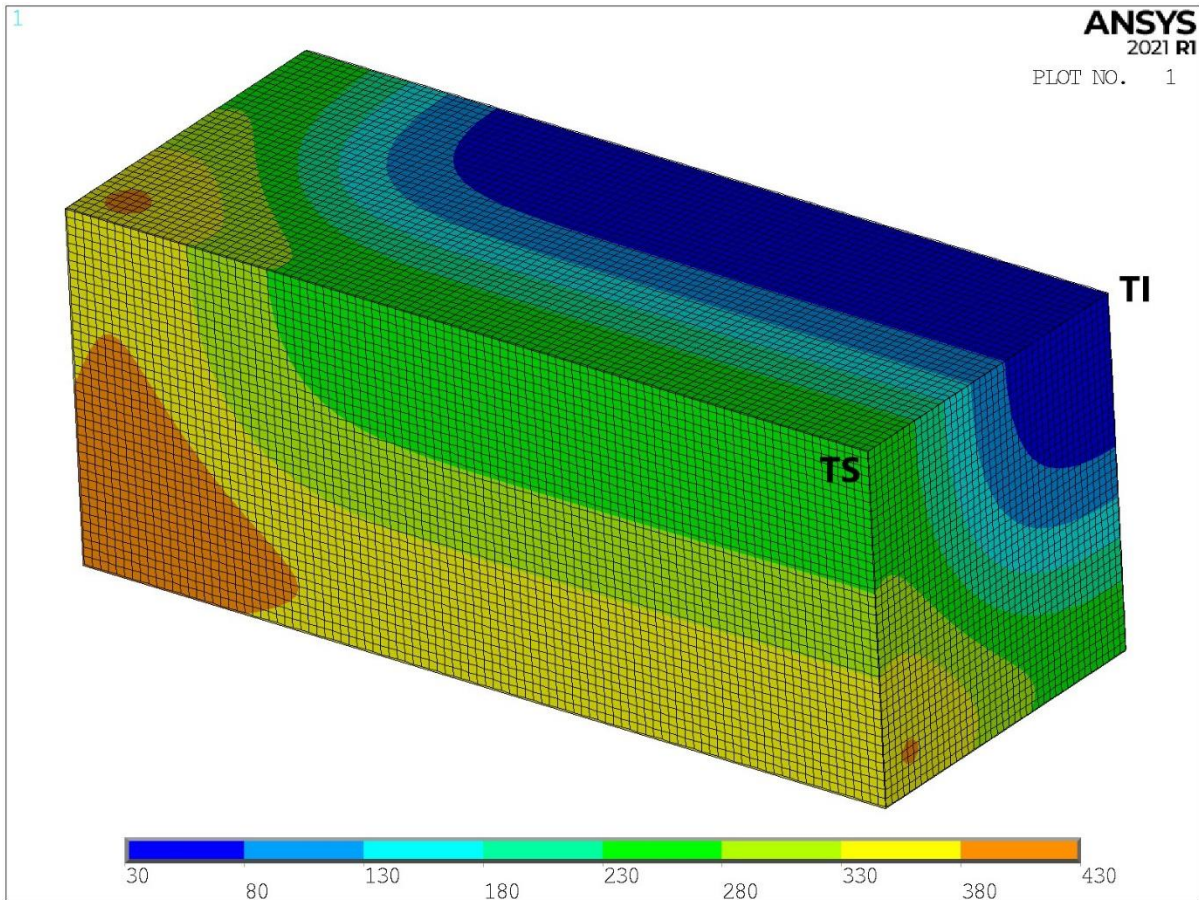


Figure 3. Temperature field of the waste product 1 h after the start of the fire, case 1.

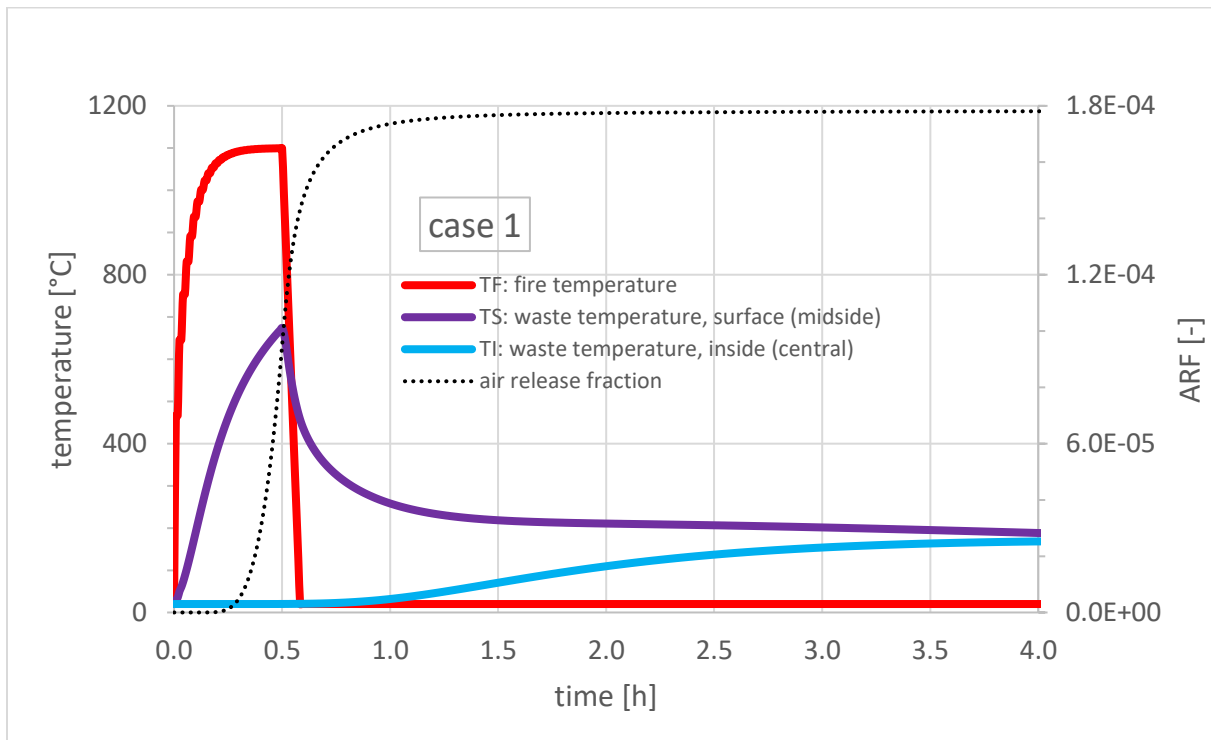


Figure 4. Temperatures and ARF for specified end of fire after 30 min.

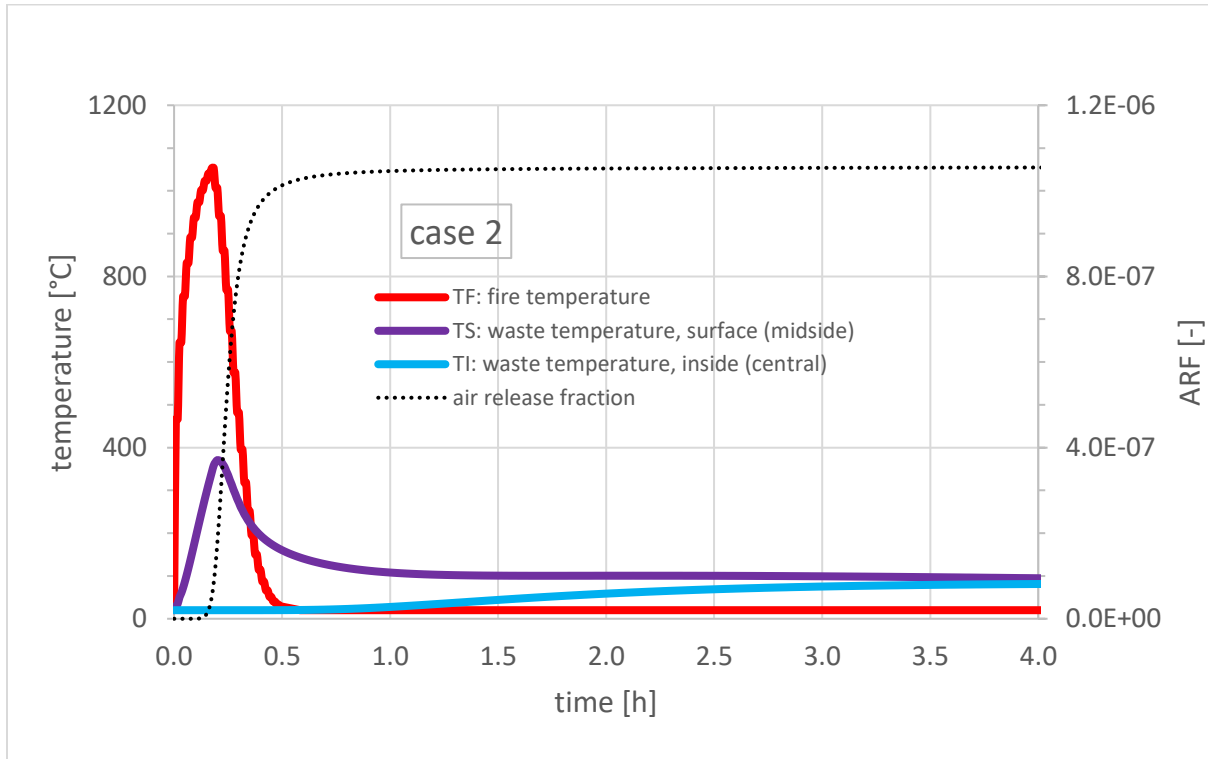


Figure 5. Temperatures and ARF considering intervention of the public fire department

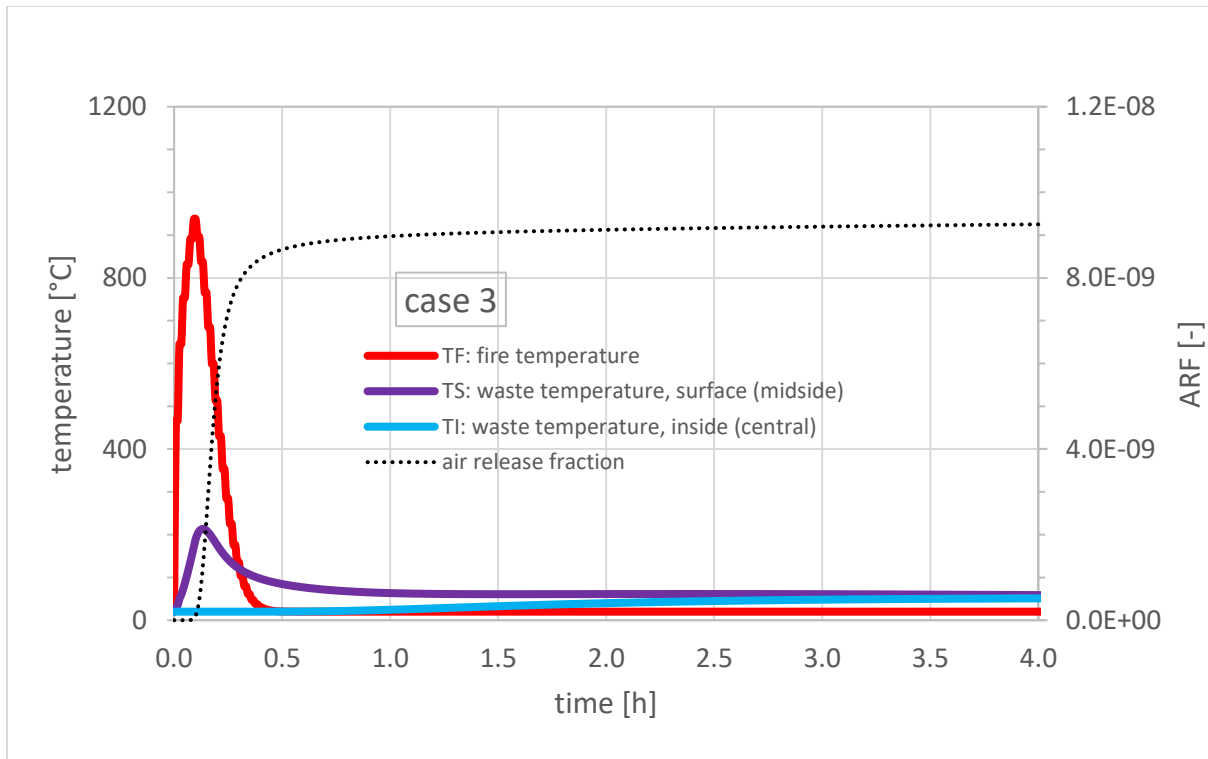


Figure 6. Temperatures and ARF considering intervention of the plant fire department.

## **CONCLUSION**

In the present work, we have investigated how the fire of a transport vehicle can affect the radioactive waste stored in 20' containers and which releases are possible under the assumed boundary conditions. In doing so, we assumed three different scenarios, which were differentiated on the basis of the intervention time of extinguishing measures. It turns out that a significant portion of the release occurs after the end of the pool fire, which is due to the delayed heat penetration into the interior of the waste. Thus, an early end of the fire can contribute significantly to the reduction of release not only by limiting the period of high temperatures, but also the maximum temperatures at the outer edge of the waste and the heat penetration into deeper layers. It should be noted here that the methodology and relationships presented in this paper could, in principle, be applied to other waste products. However, since the maximum release rate and the release duration strongly depend on the heat transport properties of the waste, the results presented here have to be recalculated for other waste products. Likewise, investigations that are more detailed and modelling of the fire event, e.g., by real fire tests or more complex computational models, can provide more specific values for the present boundary conditions.

## REFERENCES

- Boetsch, W. U.; Gründler, D.; Thiel, J. (2005). “*Thermal Behaviour of Radwaste / Experimental Studies*”, Waste Management Conference WM-05, Tucson, February 27 – March 3, 2005
- Brüchner, W., Büttner, U., Eich, P., Martens, R., Richter, C., Schrödl, E., Sentuc, F.-N., Thielen and H. (2013). „*Vertiefung und Ergänzung ausgewählter Aspekte der Abfalltransportrisikoanalyse für die Standortregion der Schachanlage Konrad*“, GRS Abschlussbericht zum Vorhaben 3607R02600, Arbeitspaket 1, Teilaufgaben 11-14, Februar 2013
- Bundeministerium des Innern BMI (1983), *Störfall-Berechnungsgrundlagen für die Leitlinien des BMI zur Beurteilung der Auslegung von Kernkraftwerken mit DWR gemäß §28 Abs.3 StrlSchV vom 18.10.1983 (BAnz Nr. 245 vom 31.12.1983), geändert 29.06.1994 (BAnz Nr. 222a vom 26.11.1994) mit Störfallberechnungsgrundlagen zu § 49 StrlSchV*; Neufassung des Kapitels 4: Berechnung der Strahlenexposition
- Bundesamt für Strahlenschutz (2010). *Anforderungen an endzulagernde radioaktive Abfälle (Endlagerungsbedingungen, Stand Oktober 2010)* - Endlager Konrad -, SE-IB-29/08-REV-1
- Bundesamt für Strahlenschutz (2010a). *Produktkontrolle radioaktiver Abfälle, radiologische Aspekte - Endlager Konrad*, Stand Oktober 2019, SE-IB-30/08-REV-1
- Bundesamt für Strahlenschutz (2010b). *Produktkontrolle radioaktiver Abfälle, stoffliche Aspekte - Endlager Konrad*, Stand Oktober 2019, SE-IB-31/08-REV-1
- DIN EN 1991-1-2:2010-12 (2010). *Eurocode 1: Einwirkungen auf Tragwerke – Teil 1-2: Allgemeine Einwirkungen Brandeinwirkungen auf Tragwerke*
- Entsorgungskommission (ESK) (2013). “*ESK-Stresstest für Anlagen und Einrichtungen der Ver- und Entsorgung in Deutschland, Teil 2: Lager für schwach- und mittelradioaktive Abfälle, stationäre Einrichtungen zur Konditionierung schwach- und mittelradioaktiver Abfälle, Endlager für radioaktive Abfälle*“, Revidierte Fassung vom 18.10.2013
- Entsorgungskommission (ESK) (2021). Empfehlung der Entsorgungskommission *Leitfaden für die Zwischenlagerung radioaktiver Abfälle mit vernachlässigbarer Wärmeentwicklung*, revidierte Fassung vom 09.12.2021
- Gründler, D. „*Bestimmung störfallbedingter Aktivitätsfreisetzung*“, GRS Systemanalyse Konrad, Teil 3, GRS-A-1389; November 1987
- Hidaka, A.; Kudo, T.; Nakamura, T.; Uetsuka, H. (2002). “*Decrease of Cesium Release from Irradiated UO<sub>2</sub> Fuel in Helium Atmosphere under Elevated Pressure of 1.0 MPa at Temperature up to 2773 K*”, J. of Nuclear Science and Technology, Vol 39, No 7, p. 759-770, July 2002
- International Atomic Energy Agency “*Advisory Material for the IAEA Regulations for the Safe Transport of Radioactive Material (2012 Edition)*”, Specific Safety Guide IAEA SSG-26, 728
- Richter, Cornelia; Sogalla, Martin; Thielen, Harald; Martens, Reinhard (2015). „*ARTM – Atmosphärisches Radionuklid-Transport-Modell mit der graphischen Benutzeroberfläche GO-ARTM, Programmbeschreibung zu Version 2.8.0 (GO-ARTM Version 2.0)*“, Gesellschaft für Anlagen- und Reaktorsicherheit (GRS) mbH, Köln, im Auftrag des Bundesamtes für Strahlenschutz, 17.04.2015
- VDI-Guideline 3945, Part 3 (2020). “*Environmental meteorology, Atmospheric dispersion models, Particle model*”, April 2020
- Vereinigung zur Förderung des Deutschen Brandschutzes (vfdb) (2020). *Leitfaden Ingenieurmethoden des Brandschutzes*, Technischer Bericht vfdb TB 04-01, 03.2020